Effect of Coulomb scattering on low-pressure high-density electronegative discharges

E. Kawamura and C. K. Birdsall
EECS Department, University of California at Berkeley, Berkeley, California 94720, USA
(Received 10 September 2004; published 9 February 2005)

For electronegative plasmas with low gas pressure and high ion densities, we expect Coulomb collisions between positive and negative ions to dominate over collisions between ions and neutrals. We incorporated Nanbu's cumulative small-angle collision method [K. Nanbu, Phys. Rev. E, **55**, 4642 (1997)] into our one-dimensional three-velocity-component particle-in-cell code PDP1 in order to study the effect of Coulomb collisions on low pressure high density electronegative discharges. Nanbu's method treats a succession of small-angle binary collisions as a single binary collision with a large scattering angle, which is far faster than treating each individual small-angle collision. We find that Coulomb collisions between positive and negative ions in low-pressure high-density electronegative discharges significantly modify the negative ion flux, density, and kinetic energy profiles.

DOI: 10.1103/PhysRevE.71.026403 PACS number(s): 52.65.Rr, 52.50.Qt, 52.27.Cm, 52.20.Hv

I. INTRODUCTION

The current trend for plasma reactors is towards lower background gas pressure and higher plasma density. Lower gas pressures minimize ion-neutral collisions, leading to narrower ion angular distributions at the target electrode. This highly anisotropic ion flux at the target produces the sharp features with high aspect ratios required for integrated circuits. Higher plasma densities maximize the ion flux at the target electrode, leading to faster etching.

One example of a high-density plasma (HDP) reactor is an inductively coupled plasma (ICP) source. In an ICP reactor, rf power is applied to an external coil, and the resulting induced electric field drives the plasma discharge. The ICP source is attractive compared to other types of HDP sources such as electron cyclotron resonance (ECR) and helicon sources because it has a simple design, does not require dc magnetic fields, and uses rf rather than microwave power. Furthermore, unlike capacitively coupled discharges, control of the plasma density and of the ion bombarding energy can be decoupled by using two separate driving circuits: one to power the induction coil, the other to power the target electrode. As a result, the inductive discharge can operate at a low plasma potential ($\sim$10–30 V) to minimize surface damage to the wafer.

Typical industrial plasma reactors often use gases with complex chemistries (e.g., oxygen, halogen, fluorocarbons) which tend to generate discharges containing negative ions. These electronegative plasmas are not as well studied as electropositive plasmas and may have significantly different characteristics.

For a bounded plasma, the plasma potential becomes positive with respect to the walls so that in equilibrium, equal fluxes of the positive ions and the more mobile electrons reach the walls. Due to Debye shielding, most of this potential drop does not fall across the bulk plasma but is confined to spatial regions near the walls called *sheaths*. Thus, in plasma reactors, positive ions form in the bulk and fall down a sheath potential hill towards the walls. In contrast, negative ions are trapped by the positive plasma potential and cannot enter the sheaths but must be chemically destroyed within the bulk (e.g., by recombination or electron detachment). This longer residence time in the bulk increases the interactions of negative ions with other plasma species.

For low pressures and high ion densities, Coulomb scattering momentum transfer can couple the positive and negative ion flows. Within the bulk plasma, the positive ions can drag the negative ions outwards against their electric field acceleration and towards the plasma walls. However, at the sheaths, low positive ion density and strong electric field combine to decouple the positive and negative ion flows. The positive ions continue to accelerate outwards while the negative ions are accelerated inwards. Any Coulomb induced outward negative ion flow dies out before reaching the sheaths, trapping negative ions in presheath boundary layers. As a result, the negative ion density at a boundary layer can exceed its value in the bulk, leading to peaks in the negative ion density profile.

II. FLUID CODE RESULTS

Vitello [1] studied the effect of Coulomb scattering on inductive electronegative discharges using the two-dimensional (2D) fluid code INDUCT95 [2]. INDUCT95 solves several moments of the Boltzmann equation self-consistently with Poisson's equation for the electric potential: it solves (i) the electron and ion continuity equations, (ii) the ion momentum balance equation and uses the drift-diffusion approximation for the electron flux, (iii) the electron energy balance equation. This code assumes Maxwellian velocity distributions and a fixed ion temperature. Inductive heating is calculated from a time-averaged solution of Maxwell's equations.

Vitello studied inductive chlorine discharges with high density ($\gg 10^{16}$ m^{-3}), low pressure (5–50 mTorr), and low plasma potential ($\approx$10–30 eV). He found that for a fixed inductive power, the effect of Coulomb scattering on Cl^- ion density and flux profiles increased with decreasing neutral pressure. (Increasing inductive power had the same effect as decreasing neutral pressure.) He observed the coupling of the

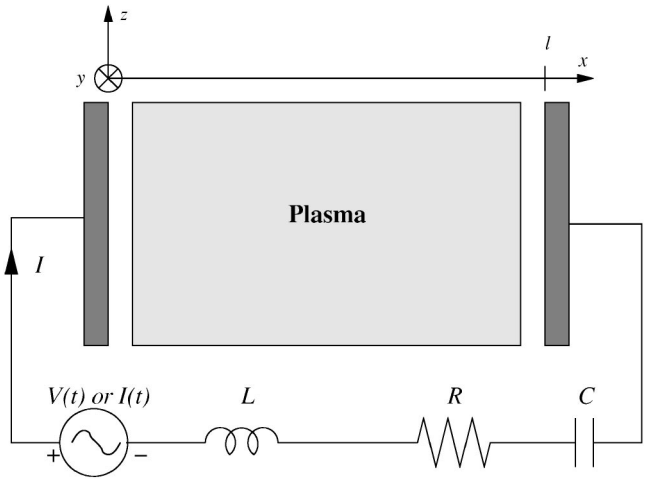

FIG. 1. Model for the plasma device code PDP1, showing all of the elements of a whole device, with the plasma between the electrodes and the external driving circuit outside, all solved simutaneously. From Verboncoeur *et al.* [4].

negative and positive ion fluxes due to Coulomb scattering momentum transfer. He noted the formation of presheath boundary layers in which the Coulomb induced outward Cl^- ion flow stagnated, trapping Cl^- ions in a presheath boundary layer and causing peaks in the Cl^- ion density profile. These density peaks became more pronounced at lower pressures. For his lowest pressure (5 mTorr) case, Vitello observed turbulence, with large spatial and temporal variations in the Cl^- ion density.

Vitello noted that further studies should be made on the effect of Coulomb scattering on ions due to the restrictions of the fluid code INDUCT95. The large observed spatial variations in ion density and flux tend to invalidate the code's assumption of fixed ion temperature. Also, the code ignores the energy dependence of certain cross sections such as ion-ion neutralization, and ion-neutral elastic scattering and charge exchange. Finally, though fluid codes may typically run faster than particle codes, they make questionable assumptions about ion and electron velocity distributions and ignore kinetic effects. Thus a kinetic approach to the study of the effect of Coulomb collisions on electronegative discharges is desirable.

III. PIC AND COULOMB MODEL

A. PIC-MCC model

Particle-in-cell (PIC) simulations can obtain the fields and the density and flux profiles self-consistently from first principles without making any assumptions about the electron and ion temperatures or their velocity distributions. Electron-neutral, ion-neutral, and certain electron-ion and ion-ion collisions (such as recombination and electron detachment) can be included in PIC simulations by combining PIC methods with Monte Carlo collisions (MCC). A detailed reference to the PIC-MCC model used in our code is provided by Vahedi and Surendra [3].

Figure 1 shows the bounded plasma model used in our planar one-dimensional three-velocity component (1D3V) PIC-MCC code PDP1 [4,5]. The metal electrodes at $x=0$ and $x=l$ bound the plasma region and have surface charge, both induced by the fields in the plasma and from charges deposited from the external circuit. By "1D3V," we mean one-dimensional displacement (1D) with three velocity components (3V). Each computer particle is a "superparticle" which represents 10^6-10^9 real particles (electrons or ions). The simulation must run with a sufficient number of particles in order to minimize the discrete particle noise. For each particle, PDP1 keeps track of its displacement in the axial (x) direction and its velocity components in the axial (x) and perpendicular (y and z) directions.

In a typical electrostatic PIC-MCC simulation, for each time step:

1. The charge density $\rho(x)$ is obtained by a linear weighting of the particles to the spatial grid.
2. $\rho(x)$ is used in Poisson's equation to solve for the electric field $E(x)$.
3. $E(x)$ is linearly weighted back to each particle position in order to determine the force on each particle.
4. The Newton-Lorentz equations of motion are used to advance the particles to new positions and velocities.
5. The boundaries are checked, and out of bounds particles are removed.
6. A Monte Carlo collision handler checks for collisions and adjusts the particle velocities accordingly.

However, this PIC-MCC model does not accurately simulate Coulomb interactions within a cell. Recall that we obtain the charge density by a linear weighting of the particles to the spatial grid. This linear interpolation reduces the level of statistical noise in a simulation and also leads to the appearance of particles that are one grid cell wide. Phenomena with wavelength larger than a cell size are not changed, but any shorter wavelength phenomena such as "close-in" (within a cell) Coulomb collisions are damped out [6,7]. This omission is acceptable for conventional reactive ion etching (RIE) reactors which operate at relatively high pressure ($\sim$ few hundred mTorr) and low plasma density ($\leqslant 10^{16}$ m^{-3}). But, in order to study the new HDP reactors, we need to incorporate a close-in Coulomb collision model into our PIC-MCC code.

B. Takizuka and Abe model

Takizuka and Abe [8] proposed a binary collision model for plasma simulations with particle codes. The main steps of this model are summarized below:

1. The plasma is divided into spatial cells with width $\Delta x \sim \lambda_D$ (the electron Debye length). This ensures that the change in plasma properties across each cell is small. It also allows us to neglect Coulomb collisions between particles in different cells.
2. The initial positions and velocities of the particles are set up.
3. The time step Δt must be small enough so that the probability of a particle colliding more than once per Δt is low.
4. The particle motion and the collisions are assumed to

be decoupled over the time step Δt, and the particles are advanced by the usual PIC method.

5. The particles are sorted in memory via cell location. That is, the cells are numbered and the particles are arranged in memory by the cell number.

6. Randomly pair off particles in each cell. The model neglects the separation of particles within a cell.

7. The changes in the velocities of each pair of particles due to a binary collision in the time step Δt are calculated and the particle velocities are adjusted accordingly.

8. The cycle is repeated until the end of the simulation.

The Takizuka and Abe model can be incorporated into PIC-MCC codes in a straightforward manner, but it is computationally intensive since each small angle binary collision is calculated one by one.

C. Nanbu model

Nanbu [9] proposed a revised binary collision model in which a succession of small-angle binary collisions was grouped into a single binary collision with a large cumulative deflection angle. The probability density function for this cumulative deflection angle depended on the simulation time step Δt. Thus the time step Δt does not have to be small enough to resolve each small-angle binary collision. Instead, the time step Δt can be chosen independently (e.g., to satisfy other less stringent stability and accuracy conditions) and the cumulative scattering angles can be calculated accordingly.

How large is the cumulative scattering angle χ_N for a test particle after N small-angle Coulomb collisions with target particles? Nanbu discovered that $f(\chi_N)$ (the probability density function for χ_N) is a unique function of a parameter:

$$s = \frac{1}{2} N \langle \theta_1^2 \rangle, \tag{1}$$

where θ_1 is the deflection angle for a single small-angle collision. From Eq. (3.3.6) of the Lieberman and Lichtenberg text [10], we know that

$$\langle \theta_1^2 \rangle = 2 \left(\frac{b_0}{b_{\max}} \right)^2 \ln \left(\frac{b_{\max}}{b_0} \right), \tag{2}$$

where $b_{max} \approx \lambda_D$ is the maximum impact parameter and b_0 is the classical distance of closest approach. The number of target particles N encounterd by a test particle traveling with a relative speed v_R is given by

$$N = n_t \pi b_{\max}^2 v_R \Delta t, \tag{3}$$

where n_t is the target particle density. Plugging Eq. (2) and Eq. (3) into Eq. (1) results in the expression

$$s = n_t v_R \pi b_0^2 \ln \left(\frac{\lambda_D}{b_0} \right) \Delta t. \tag{4}$$

For small s, Nanbu found that $f(\chi_N)$ is a narrowly distributed Gaussian centered about $\chi_N = 0$. In this case, χ_N tends to be small and the test particle hardly deviates from its original path. For large s, Nanbu found that $f(\chi_N)$ approaches $1/4\pi$ (an isotropic distribution). In this case, χ_N tends to be large and the test particle is scattered significantly from its path. Because of the dependence of $f(\chi_N)$ on s, Nanbu aptly named s the *isotropy* parameter.

In order to incorporate Nanbu's model into our code, we added the following steps to the usual PIC-MCC cycle described above.

1. Sort particles in memory via cell location.
2. Randomly pair off particles in each cell.
3. For each pair, calculate the isotropy parameter s.
4. From s, find the cumulative scattering angle χ_N and adjust the particle velocities accordingly.

D. Inductive discharge model

In a typical PDP1 simulation, the metal plates at $x = 0$ and $x = l$ bound the plasma and are attached to an external driving circuit which may contain an rf voltage or current source. The discharge is sustained by capacitive coupling of the plasma with the low and high voltage electrodes. In this case, high voltages (to increase electron temperature) and high neutral pressure (to increase ionization rates) are required to produce a high density plasma.

However, we desire to simulate HDP reactors such as ICP sources which typically operate at *low* neutral pressure and *low* plasma potential. Thus we must modify PDP1 to simulate discharges with *high* ion density, *low* pressure, and *low* plasma potential.

Kouznetsov [11] proposed a simple inductive discharge model for PDP1 which we briefly summarize below:

(i) Both plates are grounded, and the electrons are subjected to a 13.56-MHz spatially uniform electric field parallel to the surface of the plates.

(ii) This electric field increases the electron velocity component parallel to the plates. Electron scattering then distributes this velocity (and energy) boost to the other components.

(iii) If a constant electric field amplitude is specified in the input deck, the simulation becomes unstable (over an rf cycle, the work done by the electric field on the electrons would not be a constant but would depend on electron number). Instead, the input deck specifies the target number of electrons in the simulation. The code then adjusts the electric field amplitude to achieve the target number of electrons. When the code reaches a steady state, both the electric field amplitude and the electron number approach a constant value.

Basically, the Kouznetsov model comes down to heating the electrons by an rf field perpendicular to the simulation axis.

IV. PDP1 SIMULATION RESULTS

By incorporating Nanbu's Coulomb collision model and Kouznetsov's inductive discharge model into our PIC-MCC code PDP1, we were able to conduct 1D3V simulations of inductive electronegative oxygen discharges. The cross sections used for the short range non-Coulomb collisions in the oxygen plasma are described in detail in Ref. [3]. Unlike Vitello's INDUCT95 chlorine discharge model, the PIC-MCC oxygen discharge model includes the energy dependence of the cross sections for ion-ion neutralization and ion-neutral elastic scattering and charge exchange.

The charged particle species in our oxygen model consist of electrons, positive O_2^+ ions and negative O^- ions. As with all neutrals in our PIC codes, the O_2 molecules are assumed to form a uniform Maxwellian background gas at constant temperature and pressure. We assumed a distance between plates of $l=0.06$ m and a cross-sectional plate area of $A=0.01$ m^2. For our inductive discharge simulations, we chose an initial target electron density of $n_e=10^{17}$ m^{-3}. (This is similar to fixing the inductive power.) We assumed a background O^2 gas at room temperature (0.026 V) with pressure varying from $p=10-100$ mTorr. For each observed pressure p, we ran two PIC-MCC simulations: one with the Coulomb collisions turned completely off, and one with the ion-ion Coulomb collisions between the O_2^+ and O^- ions turned on. As a result, we were able to directly observe the effects of the Coulomb collisions between positive and negative ions on the oxygen discharges.

Kouznetsov's inductive discharge model required us to ground the plates. Thus the expected value of the plasma potential is the sheath potential drop Φ_w between a plasma and a floating wall:

$$\Phi_w = T_e \ln\left(\frac{M_i}{2\pi m_e}\right)^{1/2}, \tag{5}$$

where T_e is the electron temperature in units of V and M_i and m_e are the positive ion and electron masses, respectively. The plasma is at a higher potential than the walls so that in equilibrium equal fluxes of the heavy positive ions and the light electrons reach the walls. For oxygen discharges, the mass of the O_2^+ ion $M_i=32$ amu so that $\Phi_w \approx 4.9T_e$. In each of our simulations, the bulk electron temperature was about 3 V, leading to an expected plasma potential of about 15 V. All our simulations with Coulomb collisions turned on (C) or off (NC) showed a plasma potential close to this expected value (see, for example, Fig. 2). Due to Debye shielding, most of the potential drop does not penetrate the bulk but occurs near the walls at the sheaths. This positive plasma potential confines negative ions in the bulk plasma while accelerating positive ions towards the walls.

The PIC-MCC code results for high density oxygen discharge simulations are similar to Vitello's fluid code results for high density chlorine discharges. At low pressures, the Coulomb scattering momentum transfer between the positive and negative ions in the discharge significantly modify the negative ion density and flux. Figure 3 shows the O_2^+ (left column) and O^- (right column) density profiles at various pressures with the Coulomb collisions turned on (C, black) and off (NC, dotted). For the lower pressures, Coulomb scattering appears to create presheath boundary layers in which the O^- ion density $n_-(x)$ exceeds its value in the bulk plasma. At higher pressures, the ion-neutral collisions begin to dominate over the ion-ion Coulomb scattering, and we no longer observe these peaks in the negative ion density.

We obtain a better understanding of the effect of Coulomb scattering on the low pressure discharges by observing the ion fluxes. Figure 4 shows the O_2^+ (left column) and O^- (right column) flux profiles at $p=10$ and 20 mTorr for Coulomb collisions turned on (C, black) and off (NC, dotted).

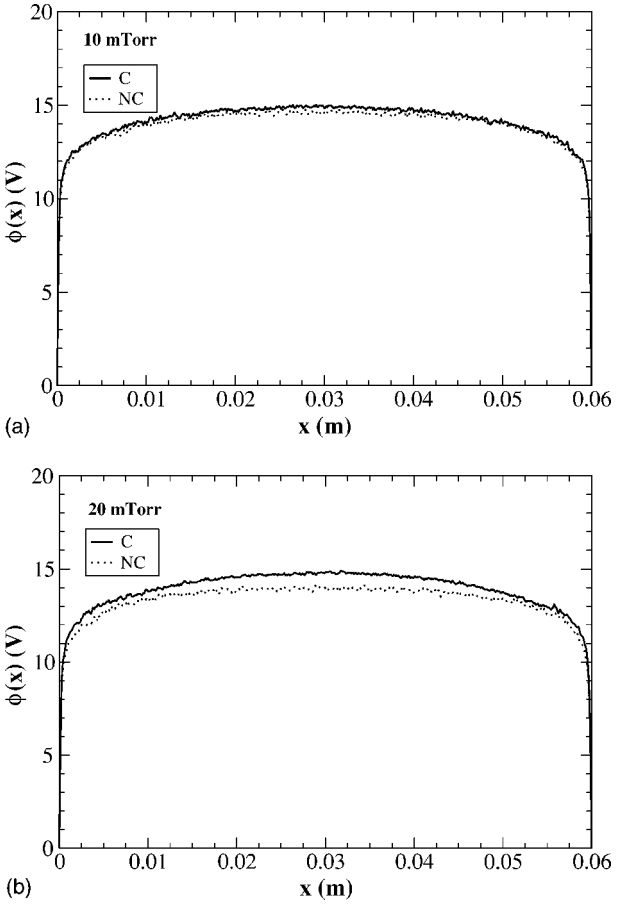

FIG. 2. PIC-MCC simulation results showing the potential $\phi(x)$ for 10- and 20-mTorr oxygen discharges with Coulomb collisions turned on (C, black) and off (NC, dotted). Note that, in all cases, the potential drop between the bulk plasma and the plates is close to the expected value of 15 V.

The Coulomb collisions do little to change the positive ion flux $\Gamma_+(x)$. The O_2^+ ions continue to fall freely down the potential hill from the center of the discharge to the walls. However, the Coulomb scattering appears to significantly modify the negative ion flux $\Gamma_-(x)$. In the absence of Coulomb scattering, the negative ions always follow their electric field force direction and flow inwards away from the sheaths and towards the center. In the presence of Coulomb scattering, spatial regions develop in the plasma where the negative ions travel against their field force and towards the walls. But once reaching the sheaths, these negative ions follow their field force again and are accelerated inwards.

Coulomb scattering momentum transfer couples the positive and negative ion flows so that positive ions can drag negative ions against their electric field acceleration and towards the walls. At the sheaths, however, the field becomes strong enough and the positive ion density low enough to decouple $\Gamma_+(x)$ from $\Gamma_-(x)$. Positive ions continue to accelerate towards the walls while the negative ions are accelerated back towards the center. So, the Coulomb induced outward flow of negative ions in the bulk dies out before reaching the sheaths. This traps negative ions in a presheath boundary layer and leads to the observed peaks in the negative ion density profile.

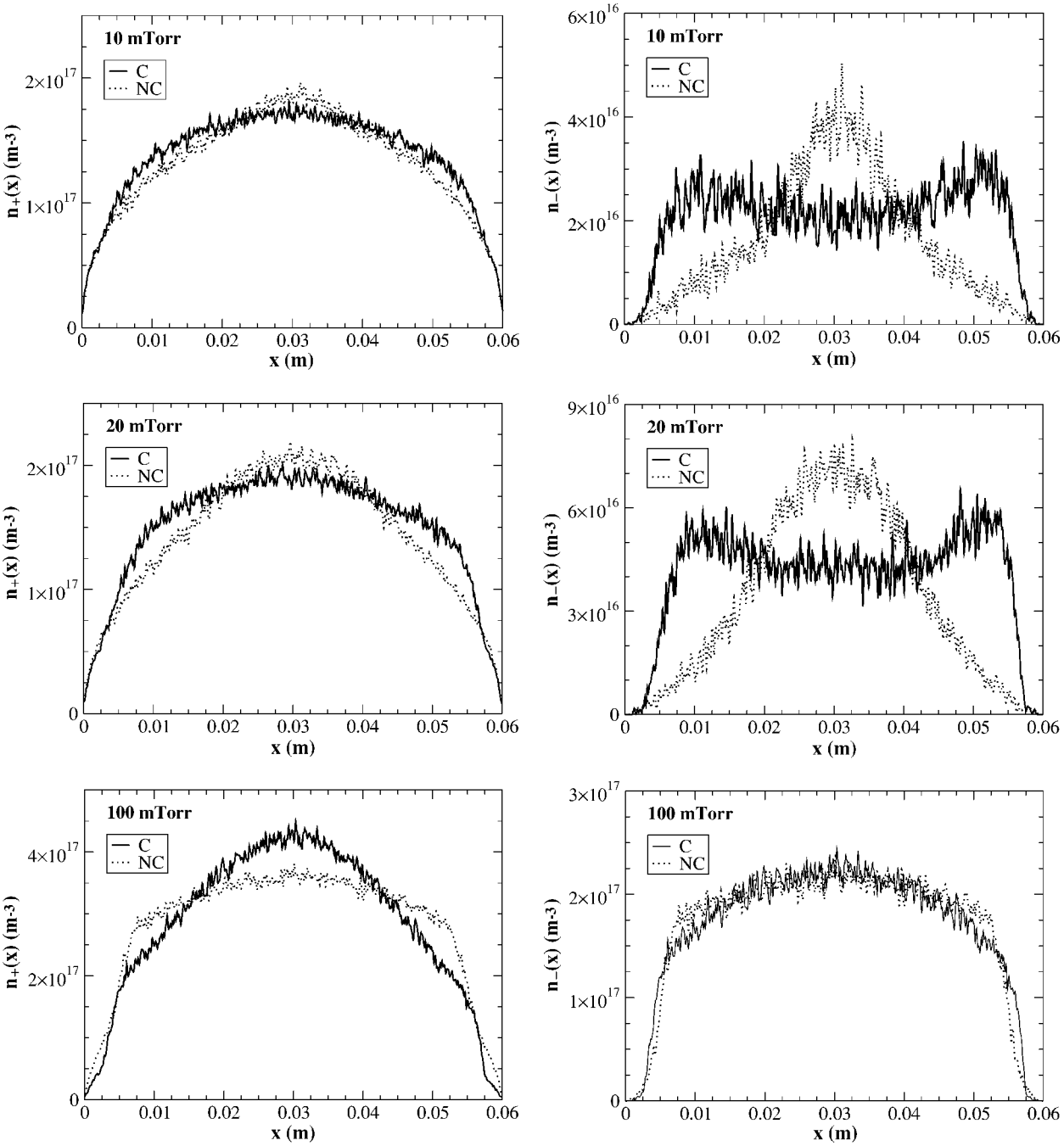

FIG. 3. PIC-MCC simulation results showing O_2^+ density $n_+(x)$ (left column) and O^- density $n_-(x)$ (right column) for 10–100-mTorr oxygen discharges with Coulomb collisions turned on (C, black) and off (NC, dotted).

The modification of the negative ion flow due to Coulomb scattering also affects the negative ion kinetic energy profiles. Figure 5 shows the average kinetic energy profiles of the O_2^+ (left column) and O^- (right column) ions at $p=10$ and 20 mTorr with Coulomb collisions turned on (C, black) and off (NC, dotted).

Coulomb scattering does not significantly affect the O_2^+ kinetic energy profile. Recall that the O_2^+ ions always follow the electric field and are constantly accelerated outwards from the center of the discharge to the walls. Thus the O_2^+ kinetic energy is low in the bulk where the field is small due to Debye shielding, and it increases rapidly at the sheaths due to the steep sheath potential drops.

Recall that the electric field accelerates O^- ions away from the sheaths and towards the center. So, in the absence of Coulomb scattering, we expect the O^- kinetic energy to be highest at the sheaths where the field is strong and gradually decline towards the center where the field is small. However, recall that in the bulk plasma, where the O_2^+ ion density is high and the field is small, Coulomb scattering momentum transfer can cause the O_2^+ ions to drag the O^- ions towards the walls. In this case, we expect the O^- kinetic energy to

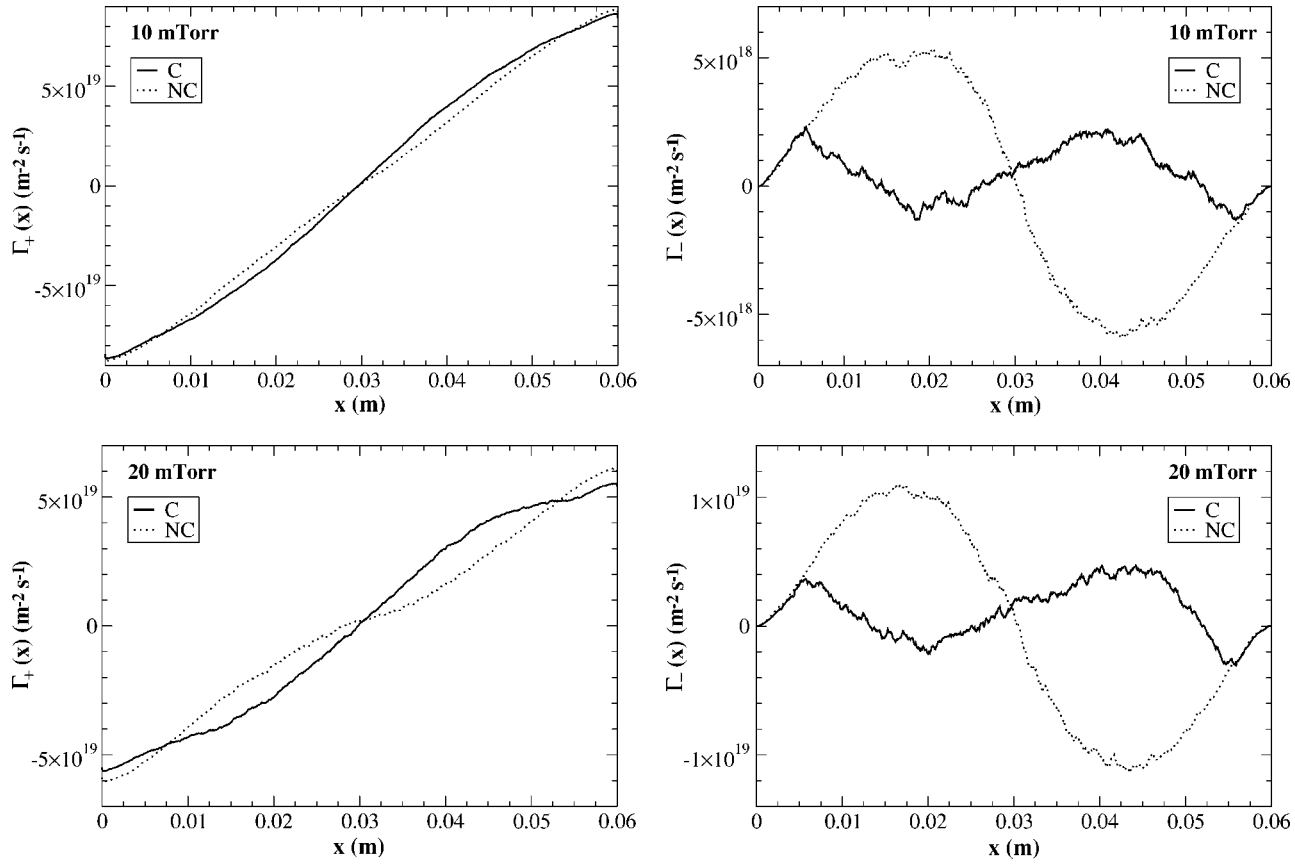

FIG. 4. PIC-MCC simulation results showing O_2^+ flux $\Gamma_+(x)$ (left column) and O^- flux $\Gamma_-(x)$ (right column) for 10 and 20 mTorr oxygen discharges with Coulomb collisions turned on (C, black) and off (NC, dotted).

decline abruptly from its high at the sheaths as soon as the O^- ions enter the presheath boundary and encounter this opposing drag force. Figure 5 confirms our expectations.

V. ANALYTICAL MODELS

In Ref. [1], Vitello introduces a simple but highly informative plasma model in order to understand the effect of ion-ion Coulomb scattering on negative ion flow. He assumes a plasma consisting of one species each of positive ions, negative ions, and neutrals; all the species have the same mass m, and all the ion species have the same ion-neutral collision frequency ν_n. Then, in regions where the pressure and velocity gradients can be neglected (i.e., away from the sheaths), the steady-state momentum balance equations for the positive and negative ions can be approximated by

$$0 = \frac{e\mathbf{E}}{\mu} - \nu_n \mathbf{v}_+ - \nu_{C+}(\mathbf{v}_+ - \mathbf{v}_-) \tag{6}$$

and

$$0 = -\frac{e\mathbf{E}}{\mu} - \nu_n \mathbf{v}_- - \nu_{C-}(\mathbf{v}_- - \mathbf{v}_+), \tag{7}$$

where $\mu = m/2$ is the reduced mass and ν_{C+} and ν_{C-} are the positive ion and negative ion Coulomb collision frequencies, respectively. Equations (6) and (7) can be solved simultaneously to obtain the mean ion velocities,

$$\mathbf{v}_+ = \frac{e\mathbf{E}}{\mu\nu_n}\left(\frac{\nu_{C-} - \nu_{C+} + \nu_n}{\nu_{C-} + \nu_{C+} + \nu_n}\right) \tag{8}$$

and

$$\mathbf{v}_- = -\frac{e\mathbf{E}}{\mu\nu_n}\left(\frac{-\nu_{C-} + \nu_{C+} + \nu_n}{\nu_{C-} + \nu_{C+} + \nu_n}\right). \tag{9}$$

When ion-neutral scattering dominates over ion-ion Coulomb scattering (i.e., $\nu_n \gg \nu_{C+}$ and $\nu_n \gg \nu_{C-}$), the mean ion velocities approach their Ohmic drift values: $\mathbf{v}_+ = e\mathbf{E}/(\mu\nu_n)$ and $\mathbf{v}_- = -e\mathbf{E}/(\mu\nu_n)$. The ions flow in the same direction as their electric field acceleration. This is what we observed in our PIC-MCC simulations with Coulomb collisions turned off (NC) and in our higher pressure PIC-MCC simulations.

Next, consider a case where ion-ion Coulomb scattering dominates over ion-neutral scattering (i.e., $\nu_{C+} \gtrsim \nu_n$ or $\nu_{C-} \gtrsim \nu_n$). Note that the ion Coulomb frequencies are proportional to their respective target densities: $\nu_{C+} \propto n_-$ and $\nu_{C-} \propto n_+$. For discharges with one positive and one negative ion species each, the quasineutrality condition in the bulk ($n_+ = n_e + n_-$) ensures that $n_+ > n_-$. If $n_+ \gg n_-$, then $\nu_{C-} \gg \nu_{C+}$, and the mean ion velocities approach $\mathbf{v}_+ = e\mathbf{E}/(\mu\nu_n)$ and $\mathbf{v}_- = e\mathbf{E}/(\mu\nu_n)$. The positive ions continue to flow with the field while the negative ions reverse direction. This is what we

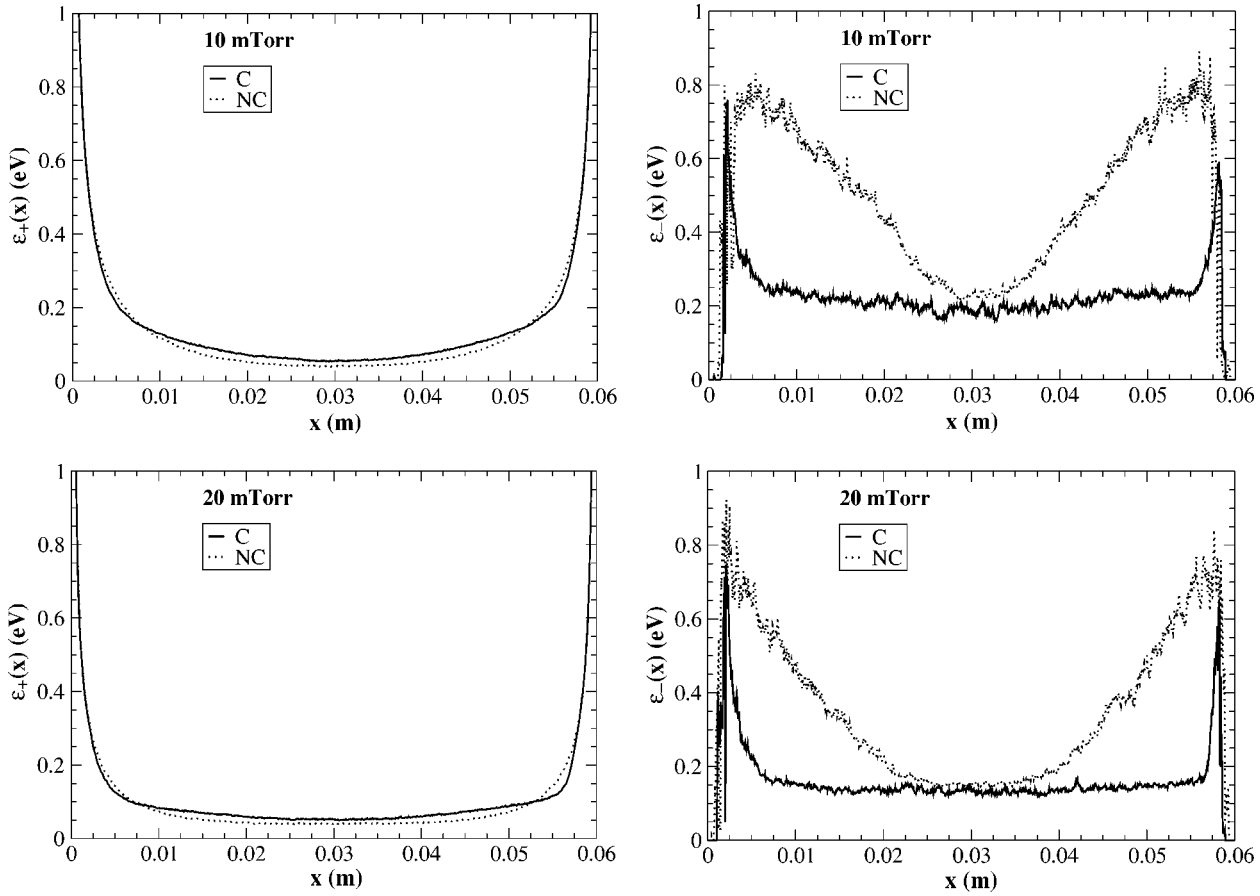

FIG. 5. PIC-MCC simulation results showing O_2^+ average kinetic energy profile $\varepsilon_+(x)$ (left column) and O^- kinetic energy profile $\varepsilon_-(x)$ (right column) for 10- and 20-mTorr oxygen discharges with Coulomb collisions turned on (C, black) and off (NC, dotted).

observed in our PIC-MCC simulations at low pressure with Coulomb collisions turned on (C).

Deutsch and Räuchle [12] conducted a detailed analysis of ion flow in electronegative discharges and found a similar result. The plasma model used by Deutsch and Räuchle is similar to Vitello's but allows the positive ion mass m_+ to differ from the negative ion mass m_-. They find that for n_- less than a critical value n_-^*, Coulomb scattering momentum transfer from the positive ions to the negative ions in the bulk plasma exceeds the electrostatic force and the retarding force from ion-neutral collisions. As a result, the negative ions flow outwards with the positive ions towards the walls. For $n_- > n_-^*$, the electrostatic force dominates and collisions have only retarding effects. As a result, the negative and positive ions flow in opposite directions. Deutsch and Räuchle calculated the critical ion density for their plasma model and found it to be

$$n_-^* = \left(1 - \frac{\nu_n m_+}{\nu_{C-} m_-}\right) n_+. \tag{10}$$

Note that for the very low-pressure high-plasma-density case in which $\nu_n \ll \nu_{C-}$, the equation reduces to $n_-^* = n_+$. Then, $n_- < n_-^*$ is always satisfied due to the quasineutrality condition, and negative ions will flow with the positive ions towards the walls. For the other limiting case of very high pressure and low plasma density in which $\nu_n \gg \nu_{C-}$, it is clear from Eq. (10) that $n_-^* < 0$. Then, $n_- > n_-^*$ is always satisfied, and the negative and positive ions will flow in opposite directions. This is consistent with our PIC-MCC simulation results.

VI. CONCLUSION

Our 1D3V PIC-MCC simulations of low-pressure high-density oxygen discharges show that Coulomb collisions between the postive and negative ions in the plasma can profoundly affect the negative ion flux, density, and kinetic energy profiles. PIC codes solve for the field and particle motion self-consistently, from first principles. Unlike fluid codes (which may tend to run faster), PIC codes can obtain flux, density, and kinetic energy profiles without making any assumptions about the temperatures or velocity distributions of the particles. Also, by using Nanbu's method which combines many successive small angle binary collisions into a single binary collision with a cumulative deflection angle, we can incorporate Coulomb collisions into our PIC-MCC code PDP1 without incurring an excessive computational penalty.

For our low-pressure PIC-MCC simulations of inductive oxygen discharges, the negative ion density n_- is much less than the positive ion density n_+ (see Fig. 3). From the analysis in Sec. V, we see that this turns out to be an important

factor. Even in the low-pressure regime in which ion-ion Coulomb momentum transfer dominates over ion-neutral collisions, if n_- is greater than some critical density n_-^*, the electrostatic force will dominate and collisions will only have retarding effects. Only when $n_- < n_-^*$ does Coulomb scattering momentum transfer from the positive to the negative ions in the bulk plasma exceed the electrostatic force.

Our PIC-MCC simulation results mostly agree with Vitello's 2D fluid code simulations of high-density low-pressure inductive chlorine discharges. Like Vitello, we saw the peaks in the negative ion density profile caused by the Coulomb induced coupling of the positive and negative ion flows. However, the sharp gradients in the PIC-MCC ion density, flux and kinetic energy profiles tend to invalidate the INDUCT95 fluid code's assumption of fixed ion temperature. Also, we did not observe the unstable behavior (with large spatial and temporal variations in negative ion density) that Vitello saw for his lowest pressure (5 mTorr) case. We do not know if this is due to the limitations of the INDUCT95 fluid code discussed above (e.g., in Sec. II), or because we simply did not study lower pressure discharges (our lowest pressure case was at $p=10$ mTorr). Kouznetsov's model to mimic inductive discharges in PDP1 was attractive for its simplicity. However, we found it difficult to sustain high-density discharges with pressures below 10 mTorr when using this model. Perhaps, in the future, we can simulate more realistic inductive discharge models using 2D3V electromagnetic PIC-MCC codes.

ACKNOWLEDGMENTS

We would like to thank Professor M. M. Turner of Dublin City University for his invaluable help in incorporating Nanbu's Coulomb collision model into PDP1. We are also grateful to Professor A. J. Lichtenberg of the University of California at Berkeley and Dr. P. Vitello of LLNL for helpful discussions on electronegative plasma discharges.

[1] P. Vitello, Jpn. J. Appl. Phys., Part 1 **38**, 4283 (1999).
[2] J. D. Bukowski, D. B. Graves, and P. Vitello, J. Appl. Phys. **80**, 2614 (1996).
[3] V. Vahedi and M. Surendra, Comput. Phys. Commun. **87**, 179 (1995).
[4] J. P. Verboncoeur, M. V. Alves, V. Vahedi, and C. K. Birdsall, J. Comput. Phys. **104**, 321 (1993).
[5] C. K. Birdsall, IEEE Trans. Plasma Sci. **19**, 65 (1991).
[6] A. B. Langdon and C. K. Birdsall, Phys. Fluids **13**, 2115 (1970).
[7] H. Okuda and C. K. Birdsall, Phys. Fluids **13**, 2123 (1970).
[8] T. Takizuka and H. Abe, J. Comput. Phys. **25**, 205 (1977).
[9] K. Nanbu, Phys. Rev. E **55**, 4642 (1997).
[10] M. A. Lieberman and A. J. Lichtenberg, *Principles of Plasma Discharges and Materials Processing* (Wiley, New York, 1994).
[11] I. G. Kouznetsov, Ph.D. thesis, Department of Electrical Engineering and Computer Sciences, University of California at Berkeley, 1997.
[12] R. Deutsch and E. Räuchle, Phys. Rev. A **46**, 3442 (1992).